Structure of high-spin states in ^{91}Sr and ^{92}Sr

E. A. Stefanova,[1,2,*] M. Danchev,[3] R. Schwengner,[2] D. L. Balabanski,[3,4] M. P. Carpenter,[5] M. Djongolov,[4] S. M. Fischer,[5] D. J. Hartley,[4] R. V. F. Janssens,[5] W. F. Mueller,[6] D. Nisius,[5] W. Reviol,[7] L. L. Riedinger,[4] and O. Zeidan[4]

[1]*Institute for Nuclear Research and Nuclear Energy, BAS, 1784 Sofia, Bulgaria*

[2]*Institut für Kern- und Hadronenphysik, Forschungszentrum Rossendorf, D-01314 Dresden, Germany*

[3]*Faculty of Physics, University of Sofia, 1164 Sofia, Bulgaria*

[4]*Department of Physics and Astronomy, University of Tennessee, Knoxville, Tennessee 37996*

[5]*Physics Divison, Argonne National Laboratory, Argonne, Illinois 60439*

[6]*NSCL, Michigan State University, East Lansing, Michigan 48824*

[7]*Chemistry Department, Washington University, St. Louis, Missouri 63130*

(Received 10 October 2001; published 4 March 2002)

The nuclei ^{91}Sr and ^{92}Sr were produced at high spin as fission fragments following the fusion reaction ^{36}S + ^{159}Tb at 165 MeV. γ rays were detected with the Gammasphere array. The level schemes of ^{91}Sr and ^{92}Sr were extended up to $E \approx 6$ MeV and $E \approx 8$ MeV, respectively. Level structures in ^{91}Sr and ^{92}Sr were interpreted in shell-model calculations performed in the configuration space $(0f_{5/2}, 1p_{3/2}, 1p_{1/2}, 0g_{9/2})$ for the protons and $(1p_{1/2}, 0g_{9/2}, 1d_{5/2})$ for the neutrons. Negative-parity states in the yrast sequences are described in these calculations by coupling 3^- proton excitations to the unpaired $1d_{5/2}$ neutrons. A possible reduction of the gap between the proton $1p_{3/2}$ and $1p_{1/2}$ orbitals in ^{92}Sr is discussed.

DOI: 10.1103/PhysRevC.65.034323 PACS number(s): 23.20.Lv, 25.85.Ge, 27.50.+e

I. INTRODUCTION

The Sr isotopes lying between the quasidoubly magic nuclide ^{88}Sr with $N=50$ and the $1d_{5/2}$ neutron subshell closure in the nuclide ^{94}Sr with $N=56$ represent one of the regions of very low collectivity in the nuclear chart. Almost constant $B(E2, 2_1^+ \rightarrow 0_1^+)$ values of ≈ 8 W.u. and 13 W.u. (W.u. denotes Weisskopf units) were found for $^{90-94}$Sr ($N=52$–56) and ^{96}Sr ($N=58$), respectively [1]. Even lower values were reported for $^{92-98}$Zr ($N=52$–58), whereas at $N=60$ a strong ground state deformation of $\beta_2 \approx 0.4$ in both isotopic chains was found [2]. The unexpectedly low $B(E2)$ values were proposed to be due to subshell closures of low-j orbitals at $Z=38,40$ and $N=56,58$ that stabilize spherical configurations [1]. While the energies of the 2_1^+ states in the even Zr isotopes increase from 919 keV at $N=54$ (^{94}Zr) to 1750 keV at the subshell closure at $N=56$ (^{96}Zr), the energies of the 2_1^+ states in the even Sr isotopes with $N=52$–58 remain almost constant at about 800 keV. The fact that the energy of the 2_1^+ state at the $N=56$ subshell closure in ^{94}Sr does not reach the order of the energy of the 2_1^+ state (1836 keV) at the $N=50$ shell closure in ^{88}Sr was related to a quenching of the $1p_{1/2}$-$1p_{3/2}$ proton spin-orbital splitting due to the neutron-proton interaction, as neutrons are added to the $1d_{5/2}$ neutron orbital [3]. If this is valid, then the question arises whether such a quenching occurs gradually between $N=50$ and $N=56$ or whether it appears suddenly at $N=56$. No apparent reduction of the gap between the proton $1p_{3/2}$ and $1p_{1/2}$ orbitals was found for ^{90}Sr [4]. The question remains still open, however, for ^{91}Sr and ^{92}Sr.

The nuclei ^{91}Sr and ^{92}Sr have three and four $1d_{5/2}$ neutrons, respectively, outside the shell closure at $N=50$. Thus, an onset of collective motion might be expected in these nuclei. However, small $B(E2, 2_1^+ \rightarrow 0_1^+)$ values were deduced as discussed above. High-spin states in the light neighbors ^{89}Sr and ^{90}Sr show interesting features such as multipletlike sequences as well as a vibrational-like $\Delta J=2$ level sequence in ^{90}Sr [4]. A large $B(E3)$ value of $43(^{+12}_{-7})$ W.u. was obtained for the $11/2^- \rightarrow 5/2^+$ transition in ^{89}Sr in an $(\alpha, n\gamma)$ experiment [5], suggesting relatively strong octupole collectivity. This value is higher than the experimental $B(E3)$ value of 22.61(12) W.u. deduced for the analogous $E3$ transition depopulating the 3^- state in ^{88}Sr [6]. The influence of the $0h_{11/2}$ neutron orbital on the first $11/2^-$ state in ^{89}Sr suggested in a previous (d,p) experiment [7] might be the reason for the strong $B(E3)$ value of the corresponding transition. The structure of the 5^- and 7^- states in ^{90}Sr predicted by the shell-model calculations in Ref. [4] is analogous to that calculated for the $11/2^-$ state in ^{89}Sr. The experimental energies of the corresponding $E3$ transitions are also very similar [4], which indicates a structural resemblence between these states. The investigation of ^{91}Sr and ^{92}Sr may reveal how the interplay of single-particle states, weak quadrupole vibrational-like excitations, and possible octupole vibrations behave with increasing neutron number.

High-spin states of ^{91}Sr and ^{92}Sr were recently observed for the first time in a fusion-fission experiment [8]. In the present work, we extended the level schemes of ^{91}Sr and ^{92}Sr and assigned tentative spins and parities to most of the levels.

II. EXPERIMENTAL METHODS AND RESULTS

The nuclei ^{91}Sr and ^{92}Sr were produced at high spin as fission fragments via the fusion reactions ^{36}S + ^{159}Tb at a beam energy of 165 MeV. The ^{36}S beam was delivered by

*Present address: II. Physikalisches Institut, Universität Göttingen, D-37073 Göttingen, Germany.

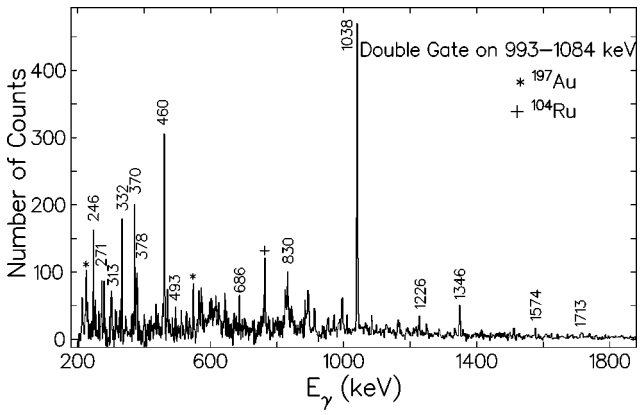

FIG. 1. Example of a doubly gated coincidence spectrum. Peaks labeled with their energy are assigned to ^{91}Sr.

the 88-Inch Cyclotron of the Lawrence Berkeley National Laboratory. The target consisted of a ^{159}Tb layer of 0.78 mg cm^{-2} thickness evaporated on to a 13 mg cm^{-2} Au backing. γ rays were detected with the Gammasphere array [9] consisting of 93 Compton suppressed Ge detectors arranged in 17 angular rings. In front of each Ge detector, Ta and Cu absorbers of 1 mm thickness were placed to attenuate x rays. A minimum of four coincident γ rays was required, and a total of about 5×10^9 events was collected. The γ-γ-γ coincidence events were sorted into an E_γ-E_γ-E_γ matrix (cube).

Doubly gated coincidence spectra were extracted using the code LEVIT8R [10]. Examples of these spectra are shown in Figs. 1 and 2 for transitions in ^{91}Sr and ^{92}Sr, respectively. The γ rays assigned to ^{91}Sr and ^{92}Sr on the basis of the present experiment are listed in Tables I and II, respectively.

A. Angular correlations of γ rays following fission

The analysis of directional correlations of coincident γ rays emitted from oriented states (DCO) was used to deduce multipole orders of the transitions and thus to assign spins to the levels they depopulate. This method is described in details in Refs. [11–13]. In the present fission experiment there are no initially oriented states. Therefore, we analyzed triple angular correlations, where one of the three coincident γ rays was used to define an orientation in space. For this purpose, we used a method corresponding to the one described in Ref. [14]. Out of all triple coincidences, only events including three γ rays fulfilling the following conditions were sorted into an E_γ-E_γ matrix:

(i) γ rays emitted in any direction were sorted along the first coordinate of the DCO γ-γ matrix.

(ii) γ rays emitted at any angle between 78.8° and 101.2° with respect to the direction of the γ ray sorted along the first coordinate were sorted along the second coordinate of the matrix.

(iii) One γ ray was required to have the energy of the ground-state transition of the nucleus of interest and to be emitted at any angle either between 0° and 41.9° or between 138.1° to 180° with respect to the γ ray sorted along the first coordinate.

We use the experimental DCO ratio defined as $R_{\rm DCO}=I_2^{\gamma_2}(\mathrm{Gate}_1^{\gamma_1})/I_1^{\gamma_2}(\mathrm{Gate}_2^{\gamma_1})$, where 1 and 2 stand for the detection angles corresponding to the first and second axis, respectively, of the DCO coincidence matrix. The quantity $I_2^{\gamma_2}(\mathrm{Gate}_1^{\gamma_1})$ denotes the coincidence intensity of a transition γ_2 measured at an observation angle 2 in a spectrum gated on transition γ_1 measured at an angle 1. The quantity $I_1^{\gamma_2}(\mathrm{Gate}_2^{\gamma_1})$ is obtained by exchanging the angles or the gating and observed transitions.

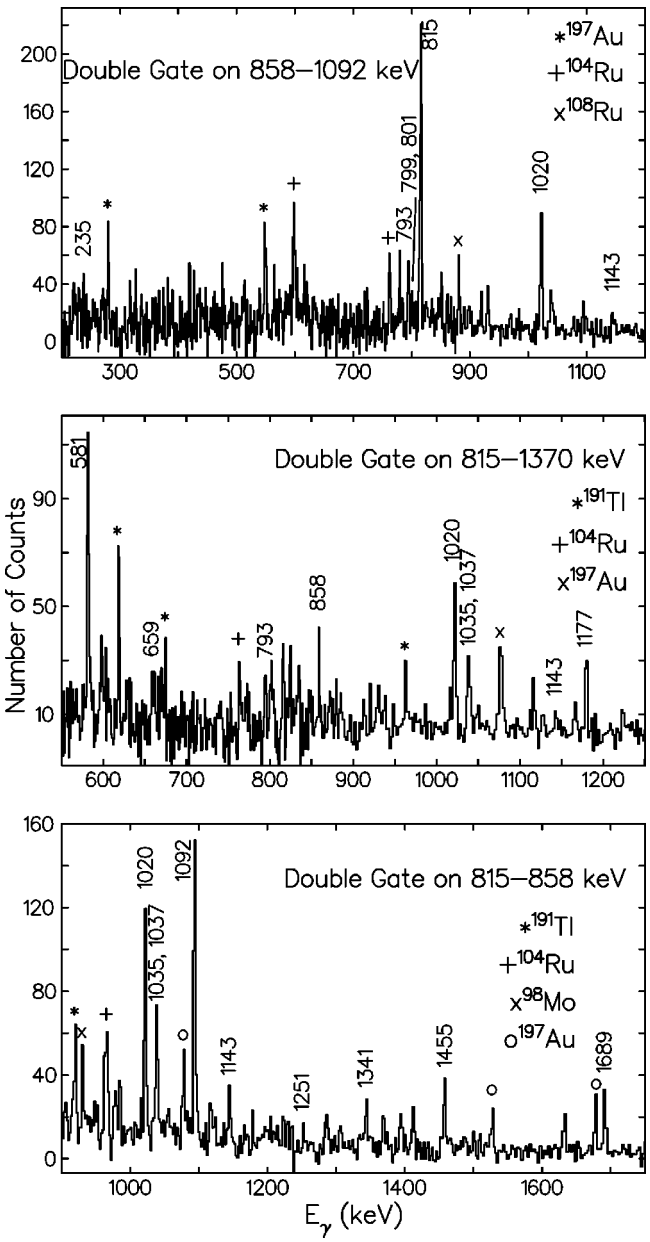

FIG. 2. Examples of doubly gated coincidence spectra. Peaks labeled with their energy in keV are assigned to ^{92}Sr.

As a consequence of condition (iii), the ground-state transition could not be used as a gating transition for the DCO analysis. Since the ranges of angles used in (ii) and (iii) are relatively large, which presumably washes the DCO ratios out, we tested this method for transitions with known multipole orders in ^{90}Sr [4] and ^{108}Pd [15]. For these transitions we deduced DCO ratios of about 0.9–1.1, if gating and observed transitions were stretched transitions of pure and

TABLE I. γ rays assigned to ^{91}Sr in the present experiment.

E_γ[a] (keV)	I_γ[b]	R_{DCO}[c]	$\sigma\lambda$[d]	J_i^π	J_f^π	E_i[e] (keV)
174.3[f]						5002.4
246.4	10.1(9)					5248.8
271.4	6.4(9)			$(17/2^-)$		3574.6
313.1	2.6(4)					5002.4
331.8	17(1)	0.94(25)[i]	$M1$	$(21/2^-)$	$(19/2^-)$	4276.6
		0.39(19)[j]				
370.2	18(1)	0.96(27)[i]	$M1$	$(19/2^-)$	$(17/2^-)$	3944.8
		0.51(32)[j]				
377.5[g]		1.05(33)[i]	$M1$ or $E1$			5002.4
459.5	30(2)			$(17/2^-)$	$(15/2^-)$	3574.6
493.1	4.9(5)	0.91(61)[i]	$M1$			5741.9
		0.51(34)[j]				
685.7[g]	6(1)					5365.0
829.7[h]	17(2)			$(19/2^-)$	$(15/2^-)$	3944.8
993.2	130(10)		$(E2)$	$(9/2^+)$	$5/2^+$	993.2
1038.3	100(5)	1.31(17)[i]	$E2$	$(15/2^-)$	$(11/2^-)$	3115.1
		1.08(11)[j]				
1083.6	115(8)	0.68(31)[j]	$(E1)$	$(11/2^-)$	$(9/2^+)$	2076.8
1225.7	8(2)				$(11/2^-)$	3303.2
1346.4	13(2)				$(15/2^-)$	4461.1
1509.1	7.1(9)				$(15/2^-)$	4624.5
1564.4	3(2)				$(15/2^-)$	4679.5
1574.2	3.9(9)				$(15/2^-)$	4689.3
1713.0	5.3(9)				$(15/2^-)$	4828.1

[a] γ-ray energy. The error is between 0.1 and 0.5 keV.
[b] Relative intensity derived from a spectrum doubly gated on the 993.2 and 1083.6 keV transitions and normalized to intensity $I_\gamma = 100$ for the 1038.3 keV transition.
[c] DCO ratio.
[d] Multipolarity compatible with the DCO ratio and the deexcitation mode.
[e] Energy of the initial state.
[f] This transition was tentatively placed in the level scheme on the basis of coincidence relations between the 246.4 and 1713.0 keV transitions.
[g] Contaminated by 378 and 686 keV transitions in the complementary fragment ^{100}Tc.
[h] Contaminated by the 830 keV transition in the complementary fragment ^{99}Tc.
[i] DCO ratio determined by gating on the 1083.6 keV ($\Delta J = 1$) transition in the present experiment.
[j] DCO ratio determined by gating on the 993.2 keV ($\Delta J = 2$) transition by using data of a previous experiment (see Sec. II A).

equal multipole order, and values of about 0.6–0.8 for pure dipole transitions gated on a stretched quadrupole transition. Consequently, inverse values of about 1.25–1.67 are expected for a quadrupole transition gated on a dipole transition. DCO ratios obtained from the present data for transitions in ^{91}Sr and ^{92}Sr are given in Tables I and II, respectively. The values for ^{91}Sr were complemented by DCO ratios deduced from our previous experiment that focused on the neighboring isotopes ^{89}Sr and ^{90}Sr [4] and contained also information about excited states in ^{91}Sr (see Table I). While the number of γ-γ-γ coincidences used to construct the level scheme of ^{91}Sr was much higher in the present experiment, the number of coincidences in the DCO matrix was drastically reduced due to conditions (ii) and (iii) and is lower than in our previous experiment. In addition, the previous data enabled gating on the 993.2 keV transition (cf. Table I), while this was used for condition (iii) in the present experiment and could not be used as a gating transition for the DCO analysis. So far, there was no experimental information about spins and parities of excited states in ^{91}Sr. A comparison of the DCO ratios of the 331.8, 370.2, and 493.1 keV transitions obtained by gating on either the 993.2 or the 1083.3 keV transitions may indicate that these γ rays have the same multipole order as the 1083.3 keV γ ray, but a smaller order than the 993.2 keV γ ray. In contrast, the 1038.3 keV transition is likely to have a multipole order that is larger than the ones of the 331.8, 370.2, and 493.1 keV transitions but equal to that of the 993.2 keV transition. These relationships suggest that the 331.8, 370.2, and 493.1 keV γ rays are dipole transitions while the 993.2 and 1038.3

TABLE II. γ rays assigned to ^{92}Sr in the present experiment.

E_γ[a] (keV)	I_γ[b]	R_{DCO}[c]	$\sigma\lambda$[d]	J_i^π	J_f^π	E_i[e] (keV)
235.4[f]	8.1(3)	0.63(17)	$(E1)$	(7^-)	(6^+)	4020.8
580.7	21.0(6)	1.50(64)[j]	$E2$	$5^{(-)}$	$3^{(-)}$	2765.2
658.9	13.6(5)			(7^-)	(5^-)	4020.8
771.3[g]	6.3(3)			(6^+)	(4^+)	3785.4
792.8[g]		1.52(46)[k,l]	$(E2)$	(7^-)	$5^{(-)}$	3558.0
798.7	7.9(6)					5726.6
800.5	4.3(3)					6527.1
814.5	149(2)		$E2$[m]	2^+	0^+	814.5
858.4	100(1)		$(E2)$	(4^+)	2^+	1672.9
1020.2[h]	26.6(7)	0.97(28)[k,l]	$(E1)$	(6^+)	(5^-)	3785.4
1035.3	10.1(6)				(7^-)	5056.1
1092.3	36.2(8)	0.56(15)	$(E1)$	(5^-)	(4^+)	2765.2
1142.5	10.3(4)				(6^+)	4927.9
1177.4	14.3(4)			(5^-)	(3^-)	3361.9
1251.4	5.8(5)				(4^+)	2924.3
1341.2[i]	5.8(3)	0.95(36)[l]	$(M1)$	(4^+)	(4^+)	3014.3
1370.0	34.2(7)			(3^-)	2^+	2184.5
1455.4	11.0(6)	1.13(57)	$(E2)$	(6^+)	(4^+)	3128.3
1689.0	5.2(3)			(5^-)	(4^+)	3361.9
1799.6	3.2(3)				(6^+)	4928.9

[a] γ-ray energy. The error is between 0.1 and 0.5 keV.
[b] Relative intensity derived from a spectrum gated on the 814.5 keV transition and normalized to intensity 100 of the 858.4 keV transition.
[c] DCO ratio determined by gating on the 858.4 keV transition except for the cases in *h* and *i*.
[d] Multipolarity compatible with the DCO ratio, the deexcitation mode, and the comparison with ^{90}Sr [4].
[e] Energy of the initial state.
[f] Contaminated by the 235 keV transition in ^{190}Tl produced with large yield.
[g] Contaminated by 771 and 793 keV transitions in ^{191}Tl produced with largest yield.
[h] Probably unresolved doublet. The intensity may be overestimated.
[i] Contaminated by the 1345 keV transition probably belonging to a nucleus produced with large yield.
[j] DCO ratio determined by gating on the 1370.0 keV ($\Delta J=1$) transition.
[k] DCO ratio determined by gating on the 1092.3 keV ($\Delta J=1$) transition.
[l] Contaminated transition. The deduced DCO ratio may not be correct.
[m] Taken from Ref. [17].

keV γ rays are quadrupole transitions. Quadrupole character may also be concluded for the 858.4 keV transition in ^{92}Sr, because the DCO ratio of 0.56(15) obtained for the 1092.3 keV transition correponds to the value expected for a dipole transition when gating on a quadrupole transition. All the DCO ratios are, however, relatively uncertain and, consequently, spin assignments were made tentatively only.

B. The level scheme of ^{91}Sr

The level scheme of ^{91}Sr deduced from the present experiment is shown in Fig. 3. This scheme is consistent with the one proposed in Ref. [8] up to the 4277 and 5002 keV states. In addition to that work, we established new levels on top of the 5002 keV state as well as new levels at 4461, 4680, 4689, and 5365 keV. In Ref. [8], spins and parities of $(9/2^+)$, $(13/2^+)$, and $(15/2^-)$ were tentatively proposed for the 993, 2077, and 3115 keV states, respectively, on the basis of systematic considerations. However, the DCO ratio of the 1083.6 keV transition deduced from the present data indicates a dipole transition (see Table I and Sec. II A). Therefore, we assign $J=(11/2)$ to the 2077 keV state. Furthermore, we tentatively assign negative parity to this state based on the observation of a $11/2^-$ state at a similar energy in the odd-mass neighbor ^{89}Sr [4,5]. Moreover, a change from positive to negative parity via an $E1$ transition was also observed in the main level sequences in the even-even isotopes ^{88}Sr [16] and ^{90}Sr [4]. Based on the quadrupole character of the 1038.3 keV transition we made the assignment $(15/2^-)$ for the 3115 keV state in agreement with the suggestion in Ref. [8]. It was not possible to deduce the DCO ratio for the 459.5 keV transition in the present or the previous experiment, because it was contaminated by the 458 keV transition from Coulomb excitation of ^{197}Au used as a target backing. Considering the $M1$ character of the 370.2 keV and 331.8

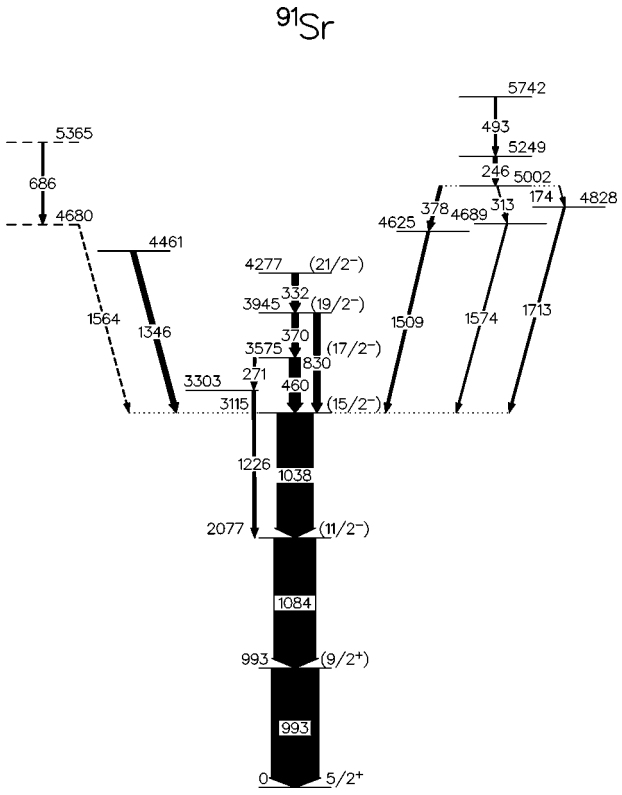

FIG. 3. Level scheme of ^{91}Sr deduced from the present experiment.

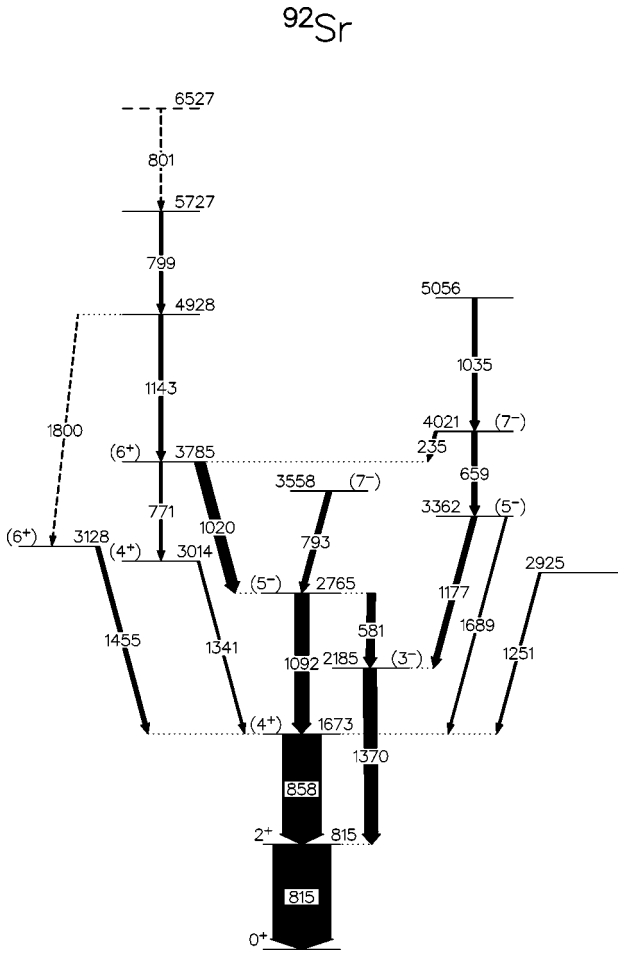

FIG. 4. Level scheme of ^{92}Sr deduced from the present experiment.

keV transitions and the observation of the 829.7 keV crossover transition, we suggest assignments of $(17/2^-)$, $(19/2^-)$, and $(21/2^-)$ for the levels at 3575, 3945, and 4277 keV, respectively.

C. The level scheme of ^{92}Sr

The level scheme of ^{92}Sr resulting from the present experiment is shown in Fig. 4. Spin and parity 2^+ of the 815 keV level have been known from previous work [17]. The level scheme was recently extended with 1673, 2185, 2765, 3785, and 4579 keV levels [8]. In the present work, we established two new sequences on top of the 3014 and 3362 keV levels, respectively. In Ref. [8], spins and parities of (4^+), (3^-), and (5^-) were assumed for the 1673, 2185, and 2765 keV states on the basis of systematic considerations. The multipole orders deduced from the present DCO analysis for the 858.4, 1092.3, and 580.7 keV transitions are consistent with these assignments. This sequence of states is very similar to the one in the even-even neighbor ^{90}Sr [4]. On the basis of the DCO ratios of the 1341.2 and 1020.2 keV transitions we tentatively assign $J^\pi=(4^+)$ and (6^+) to the 3014 and 3785 keV levels, respectively. Positive parity is suggested for these states on the basis of the similarity of the levels at 3014, 3785, 4928, 5727, and 6527 with the levels at 3269, 3764, 5055, 5923, and 6794 keV in ^{90}Sr. We do not confirm the placement of the 792.8 keV transition on top of the 3785 keV level as proposed in Ref. [8]. Instead, the 792.8 keV transition is proposed to depopulate a (7^-) state at 3558 keV. It should be noted that spins and parities 5^- or 6^+, 6^-, and 7^-, also possible from decay characteristics and a comparison with ^{90}Sr [4], cannot be totally excluded for the 3014, 3558, and 3785 keV levels, respectively, because of the large uncertanties of the DCO ratios. A transition with an energy of about 1037 keV may belong to this nucleus but could not be placed in the level scheme. The level sequence on top of the 3362 keV level resembles a sequence in ^{90}Sr [4]. Based on this resemblance, the dipole character of the 235.4 keV transition, and the deexcitation pattern of the 3362 keV level, we propose assignments of (5^-) and (7^-) for the 3362 and 4021 keV levels.

III. DISCUSSION

A. Shell-model calculations for ^{91}Sr and ^{92}Sr

Shell-model studies of nuclei with $N>50$ were focused in recent years on nuclei with $Z>40$. In these studies a model space including the $1p_{1/2}$, $0g_{9/2}$ orbitals for the protons and the $1d_{5/2}$, $2s_{1/2}$ orbitals for the neutrons has been used. The states with spins up to $J\approx 15$ could be in general well described within this model space, e.g., the $N=51$ nuclei ^{94}Tc [18] and ^{95}Ru [19], the $N=52$ nuclei ^{94}Mo [20] and ^{96}Ru [21], the $N=53$ nuclei ^{95}Mo [20] and ^{97}Ru [21], and the N

=54 nuclei ^{96}Mo [22] and ^{98}Ru [21]. For ^{95}Mo and ^{97}Ru, discrepancies found in the description of few positive-parity states were attributed to the omission of the $g_{7/2}$ neutron orbital [20]. Analogously, the description of states with spins of $J>15$ may be improved with an extended model space including the higher-lying neutron orbitals $0g_{7/2}$, $1d_{3/2}$, and $0h_{11/2}$ as well as excitations of $0g_{9/2}$ neutrons across the $N=50$ shell gap into the $1d_{5/2}$ orbital [18,20–22].

In the Sr isotopes with $Z=38$, excitations of $0f_{5/2}$ or $1p_{3/2}$ protons to the $1p_{1/2}$, $0g_{9/2}$ orbitals may contribute to the configurations of high-spin states. The model space used in our calculations includes the active proton orbitals $(0f_{5/2},1p_{3/2},1p_{1/2},0g_{9/2})$ and neutron orbitals $(1p_{1/2}, 0g_{9/2},1d_{5/2})$ relative to a hypothetic ^{66}Ni core. The restricted neutron space should be adequate for the description of states up to $J\approx 15$. Since an empirical set of effective interactions for this model space is not available up to now, various empirical interactions have been combined with results of schematic nuclear interactions applying the surface delta interaction. Details of this procedure are described in Refs. [23–26]. The effective interaction in the proton shells was taken from Ref. [27]. In that work the residual interaction and the single-particle energies of the proton orbitals were deduced from a least-squares fit to 170 experimental level energies in $N=50$ nuclei with mass numbers between 82 and 96. The data given in Ref. [28] have been used for the proton-neutron interaction between the $\pi(1p_{1/2},0g_{9/2})$ and the $\nu(1p_{1/2},0g_{9/2})$ orbitals. These data were derived from an iterative fit to 95 experimental level energies of $N=48$, 49, and 50 nuclei. The matrix elements of the neutron-neutron interaction of the $\nu(1p_{1/2},0g_{9/2})$ orbitals have been assumed to be equal to the isospin $T=1$ component of the proton-neutron interaction given in Ref. [28]. For the $(\pi 0f_{5/2},\nu 0g_{9/2})$ residual interaction the matrix elements proposed in Ref. [29] have been used. The single-particle energies relative to the ^{66}Ni core used here were derived from the single-particle energies of the proton orbitals given in Ref. [27] with respect to the ^{78}Ni core and from the neutron single-hole energies of the $1p_{1/2},0g_{9/2}$ orbitals [28]. The transformation of these single-particle energies to those relative to the ^{66}Ni core has been performed [30] on the basis of the effective residual interactions given above. The obtained values are

$$\begin{aligned}
\epsilon^{\pi}_{0f_{5/2}} &= -9.106 \text{ MeV},\\
\epsilon^{\pi}_{1p_{3/2}} &= -9.033 \text{ MeV},\\
\epsilon^{\pi}_{1p_{1/2}} &= -4.715 \text{ MeV},\\
\epsilon^{\pi}_{0g_{9/2}} &= -0.346 \text{ MeV},\\
\epsilon^{\nu}_{1p_{1/2}} &= -7.834 \text{ MeV},\\
\epsilon^{\nu}_{0g_{9/2}} &= -6.749 \text{ MeV},\\
\epsilon^{\nu}_{1d_{5/2}} &= -4.144 \text{ MeV}.
\end{aligned}$$

These single-particle energies and the corresponding values for the strengths of the residual interactions have been used to calculate level energies as well as $M1$ and $E2$ transition strengths. For the latter, effective g factors of $g_s^{\text{eff}}=0.7g_s^{\text{free}}$ and effective charges of $e_\pi=1.72e, e_\nu=1.44e$ [31], respectively, have been applied.

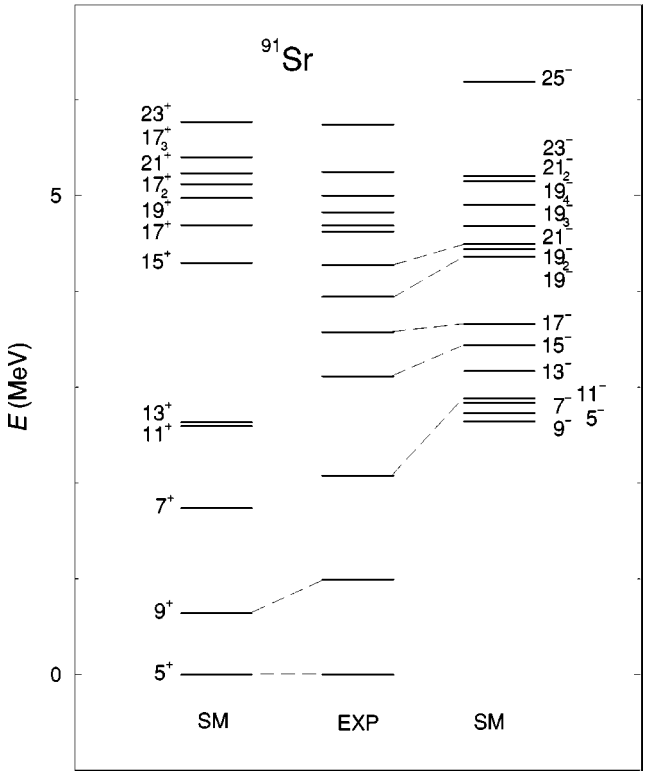

FIG. 5. Comparison of experimental with calculated level energies in ^{91}Sr. Spins are given as $2J$.

The nuclei ^{91}Sr or ^{92}Sr have ten protons and 15 or 16 neutrons, respectively, in the considered configuration space. To make the calculations feasible, a truncation of the occupation numbers has been applied. At most four protons are allowed to occupy the $(1p_{1/2},0g_{9/2})$ subshell. Two of the neutrons are assumed to occupy the $1p_{1/2}$ orbital and ten the $0g_{9/2}$ orbital while the remaining three or four appear in the $1d_{5/2}$ orbital for ^{91}Sr or ^{92}Sr, respectively. Excitations of neutrons from the $0g_{9/2}$ orbital to the $1d_{5/2}$ orbital are neglected. With these restrictions, configuration spaces with dimensions smaller than 10 300 have been obtained. The calculations were carried out using the code RITSSCHIL [32].

B. Results for ^{91}Sr

Experimental and calculated level energies in ^{91}Sr are compared in Fig. 5. The $5/2^+$ and $9/2^+$ states are mainly described by the $\nu(1d^3_{5/2})$ configuration. The $9/2^+$ state is predicted to be the first excited state in agreement with the tentative assignment of $9/2^+$ to the 993 keV level. In the $7/2^+$, $11/2^+$, and $13/2^+$ states the configuration $\pi(1p^{-1}_{3/2}1p^1_{1/2})\nu(1d^3_{5/2})$ predominates. Generating a $15/2^+$ state requires breaking a $0f_{5/2}$ proton pair resulting in a gap between the $13/2^+$ and $15/2^+$ states. The resulting main configuration of the lowest-lying $15/2^+$ state is $\pi(0f^{-1}_{5/2}1p^1_{1/2})\nu(1d^3_{5/2})$. The $17/2^+$ to $27/2^+$ states are domi-

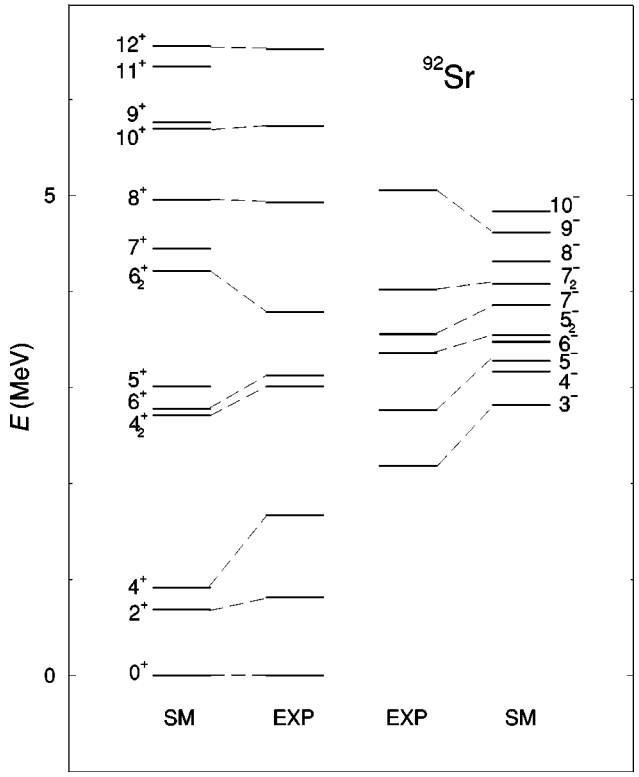

FIG. 6. Comparison of experimental with calculated level energies in ^{92}Sr.

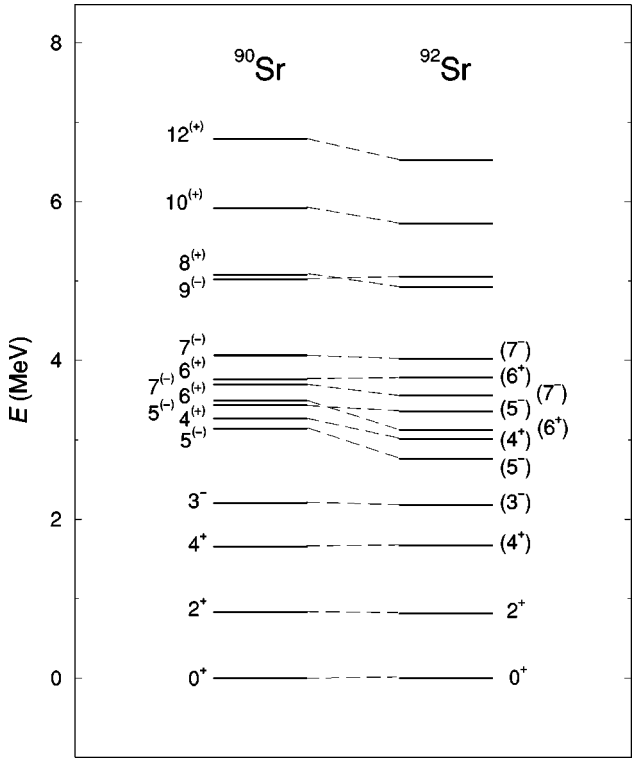

FIG. 7. Comparison of experimental level energies in ^{90}Sr and ^{92}Sr.

nated by the excitation of two protons to the $0g_{9/2}$ orbital, i.e., the configuration $\pi[(0f_{5/2}^{-2})_{J_f}(0g_{9/2}^{2})_{J_g}]\nu(1d_{5/2}^{3})_{J_d}$ with $J_f=0$, 2 , $J_g=6$, 8, and $J_d=5/2$, 9/2.

The calculated lowest-lying $5/2^-$ to $15/2^-$ states are created by lifting one $1p_{3/2}$ proton to the $0g_{9/2}$ orbital. Thus, the main configuration is $\pi(1p_{3/2}^{-1}0g_{9/2}^{1})\nu(1d_{5/2}^{3})$, except for the $13/2^-$ state which is dominated by the configuration $\pi(0f_{5/2}^{-1}0g_{9/2}^{1})\nu(1d_{5/2}^{3})$. This configuration is also the main component of the $17/2^-$ to $23/2^-$ states. We suggest the calculated $11/2^-$, $15/2^-$, $17/2^-$, $19/2^-$, and $21/2^-$ states to correspond to the experimental states at 2077, 3115, 3575, 3945, and 4277 keV, respectively. The calculated lowest-lying $11/2^-$ state is about 800 keV higher than the experimental one. A similar discrepancy was found in ^{89}Sr [4]. The calculated $11/2^-$ states in both isotopes, ^{89}Sr [4] and ^{91}Sr, are described by coupling proton configurations that correspond to the 3^- state in the core nucleus ^{88}Sr, to the neutron configurations $(1d_{5/2}^{1})_{5/2}$ and $(1d_{5/2}^{3})_{5/2}$, respectively. Consequently, both states are predicted roughly at the same energy as the 3^- state in ^{88}Sr. In a previous (d,p) study [7], an admixture of the $\nu(0h_{11/2})$ orbital to the $11/2^-$ state in ^{89}Sr was suggested. This admixture lowers the energy relative to the undisturbed one [7] and may also be the reason for the difference between the experimental and calculated $11/2^-$ states in ^{91}Sr. A similar influence of the $\nu(0h_{11/2})$ orbital may be assumed for the $15/2^-$ state, because it is calculated to include mainly the coupling of the 3^- proton excitation to the $\nu(1d_{5/2}^{3})_{9/2}$ configuration. One would therefore expect that the calculated $15/2^-$ state is about 800 keV higher than the experimental one. However, the $\nu(1d_{5/2}^{3})_{9/2}$ configuration contributing to the calculated $15/2^-$ state balances this effect partly. This configuration dominates the first $9/2^+$ state calculated to be about 350 keV lower than the experimental one. Applying this lowering to the $15/2^-$ state, the remaining difference between experimental and calculated $15/2^-$ states is about 400 keV which is consistent with the difference seen in Fig. 5.

The creation of $25/2^-$ to $27/2^-$ states requires the excitation of two protons across the shell gap at $Z=38$. Here, the main configuration is $\pi[(0f_{5/2}^{-1}1p_{3/2}^{-1})_4 1p_{1/2}^{1}0g_{9/2}^{1}]\nu(1d_{5/2}^{3})$. As can be seen in Fig. 5, the levels at 5002, 5249, and 5742 keV are better reproduced by the calculated $19/2^+$, $21/2^+$, and $23/2^+$ states than by the $21/2_2^-$, $23/2_1^-$, and $25/2_1^-$ states, respectively.

C. Results for ^{92}Sr

Calculated level energies of states in ^{92}Sr are compared with experimental ones in Fig. 6. In the calculated lowest-lying 0^+, 2^+, and 4^+ states the $\nu(1d_{5/2}^{4})_J$ configuration dominates with $J=0$, 2, and 4, respectively. Similar to ^{90}Sr [4], they form a multiplet-like sequence, whereas the experimental level spacings are rather vibrational-like. This simi- can be seen in Fig. 7, where experimental states in ^{90}Sr and ^{92}Sr are compared. The predicted $E2$ strength of the $2^+ \rightarrow 0^+$ transition in ^{92}Sr agrees well with the experimental value (see Table III). The discrepancy between the energies of the experimental and calculated 4_1^+ states may also appear

TABLE III. Experimental and calculated transition strengths in ^{92}Sr.

J_i^π	J_f^π	$B(E2)_{expt}$ [a] (W.u.)	$B(E2)_{SM}$ [b] (W.u.)
2_1^+	0_1^+	$8.0^{+4.8}_{-2.2}$ [c]	9.1

[a]Experimental reduced transition strengths in Weisskopf units (W.u.). 1 W.u.($E2$) = 23.96 e^2 fm^4.
[b]Calculated reduced transition strengths in Weisskopf units. Values of $e_\pi = 1.72e$ and $e_\nu = 1.44e$ were used for the $B(E2)$ values.
[c]Value derived from the lifetime given in Ref. [17].

in states with higher spins that include analogous configurations, i.e., the coupling of the $(1d^4_{5/2})_4$ neutrons to proton excitations. The main configuration of the first 6^+ state is $\pi(1p^{-1}_{3/2}1p^1_{1/2})_2\nu(1d^4_{5/2})_4$ with a partition of 80%, which corresponds to the main configuration $\pi(1p^{-1}_{3/2}1p^1_{1/2})_2\nu(1d^2_{5/2})_4$ of the first 6^+ state in the even-even neighbor ^{90}Sr [4]. In that nucleus, the level spacing of 1839 keV between the experimental lowest-lying 4^+ and 6^+ states is close to the energy of the experimental 2^+ state (1836 keV) in the core nucleus ^{88}Sr, which has the main configuration $\pi(1p^{-1}_{3/2}1p^1_{1/2})_2$ (see Ref. [16] and references therein). From this rough estimate, we concluded that the quenching of the proton $1p_{3/2}$-$1p_{1/2}$ spin-orbital splitting discussed in Ref. [3] is not apparent in ^{90}Sr [4]. In ^{92}Sr, however, the level spacing of 1455 keV between the first 4^+ and (6^+) states is about 400 keV lower than the corresponding value in ^{90}Sr. This may indicate a reduction of the gap between the $1p_{3/2}$ and $1p_{1/2}$ proton orbitals. Note that in the present calculation the first 6^+ state in ^{92}Sr is calculated to be about 200 keV lower than the first 6^+ state in ^{90}Sr, although the proton configurations are comparable for both states.

Main configurations of $\pi(1p^{-1}_{3/2}1p^1_{1/2})\nu(1d^4_{5/2})_{J_d}$ with $J_d=2$ and 4 are predicted for the 4^+_2 and 5^+_1 states while the 6^+_2 and 7^+_1 states are dominated by the configuration $\pi(0f^{-1}_{5/2}1p^1_{1/2})\nu(1d^4_{5/2})_4$, analogously to ^{90}Sr [4]. The second state with a tentative assignment of 6^+ at 3785 keV lies at about the same energy as the second 6^+ state in ^{90}Sr (cf. Fig. 7 and Ref. [4]). The calculated second 6^+ state in ^{92}Sr is predicted at about 3.3 MeV above the calculated 4^+_1 state, whereas the spacing between the corresponding experimental states is about 2.1 MeV only. This discrepancy resembles the findings in ^{90}Sr and might indicate the admixture of orbitals not included in the present model space as, e.g., neutron excitations of the type $\nu(1d^1_{5/2}0g^1_{7/2})$ [4]. The calculated 8^+ to 12^+ states include the excitation of two protons into the $0g_{9/2}$ orbital. The main configuration of these states is $\pi[(0f^{-2}_{5/2})_{J_f}(0g^2_{9/2})_{J_g}]\nu(1d^4_{5/2})_{J_d}$ with $J_f=0$, $J_g=6$, 8, and $J_d=0$, 2, 4. The experimental states at 4928, 5727, and 6527 keV resemble a sequence of 8^+, 10^+, and 12^+ states found in the neighbor ^{90}Sr, and are very close to the calculated 8^+, 10^+, and 12^+ states, respectively, (cf. Fig. 6). The level spacings between these possible 8^+, 10^+, and 12^+ states at 4928, 5727, and 6527 keV, respectively, are similar to the level spacings between the experimental 0^+, 2^+, 4^+ states. This suggests that the 10^+ and 12^+ states are generated by coupling the 2^+_1 and 4^+_1 states, respectively, to the 8^+ state. This feature is similar to the findings in ^{90}Sr [4] as well. The main configurations of the calculated 8^+, 10^+, and 12^+ states in ^{92}Sr support this coupling picture. As a result, the calculated 10^+ state lies below the 9^+ state which favors a $\Delta J=2$ sequence similar to the one observed in ^{90}Sr. As in that nucleus, the equidistant $\Delta J=2$ level sequence on top of the 8^+ state resembles a vibrational-like sequence, but is well reproduced in the present shell-model calculations (cf. Figs. 6 and 7).

The calculated lowest 3^-, 5^-, and 7^- states are dominated by the configuration $\pi(1p^{-1}_{3/2}0g^1_{9/2})_3\nu(1d^4_{5/2})_{J_d}$ with $J_d=0$, 2, and 4, respectively, while the lowest 4^- and 6^- states are characterized by the configuration $\pi(0f^{-1}_{5/2}0g^1_{9/2})\nu(1d^4_{5/2})_0$. In contrast to the corresponding states in ^{90}Sr and similar to the first 5^- and 7^- states in ^{92}Sr, the second calculated 5^- and 7^- states in ^{92}Sr are dominated by the configuration $\pi(1p^{-1}_{3/2}0g^1_{9/2})_3\nu(1d^4_{5/2})_4$. We assume that the calculated first 3^- and 5^- states correspond to the experimental states at 2185 and 2765 keV, respectively. The calculated first 7^- state might correspond to the experimental state at 3558 keV. The wave functions of the 3^-, 5^-_1, 5^-_2, 7^-_1, and 7^-_2 states show that these states are generated by coupling the 3^- proton excitations of the core nucleus ^{88}Sr [5,16] to the $1d^4_{5/2}$ neutron configuration. Similar to the $11/2^-$ state in ^{91}Sr (see Sec. III B), the 3^-_1 and 5^-_1 states are predicted about 600–700 keV higher than the experimental ones. A corresponding difference is expected for the 5^-_2, 7^-_1, and 7^-_2 states as well, but may partly be balanced by the $\nu(1d^4_{5/2})_4$ configuration contributing to these states because this is responsible for the lowering of the calculated 4^+ state with respect to the experiment (see above). In a previous (d,p) study, an admixture of the $\nu(0h_{11/2})$ orbital to the $11/2^-$ state in ^{89}Sr was found, which lowers its energy [7]. Such a lowering was considered as the possible origin of the discrepancies between the respective experimental and calculated states in ^{89,90}Sr [4] and ^{91}Sr (see Sec. III B) and may also be the reason for the discussed differences between experimental and calculated energies of the 3^-, 5^-, and 7^- states in ^{92}Sr. The similar energies of the 3^- and 7^- states in ^{90}Sr and ^{92}Sr (see Fig. 7) indicate similar properties of these states. However, the first 5^- state in ^{92}Sr is about 400 keV lower than the first 5^- state in ^{90}Sr [4]. The calculated 5^-_1 state in ^{92}Sr is also about 200 keV lower than the corresponding calculated state in ^{90}Sr [4]. A possible reason for this lowering may be that the calculated 5^-_1 state in ^{92}Sr includes a mixing of the configurations of the first and the second 5^- states in ^{90}Sr. The inclusion of the $0h_{11/2}$ neutron orbital as well as lifetime measurements for these states might reveal whether the configuration mixing or a possible increase of octupole collectivity is the origin for the lowering of the experimental 5^-_1 state in ^{92}Sr compared with that in ^{90}Sr.

The calculated states with higher spin are mainly described by the configuration $\pi(0f^{-1}_{5/2}0g^1_{9/2})\nu(1d^4_{5/2})_{J_d}$ with $J_d=2$ for the 8^- state and $J_d=4$ for the 9^- to 11^- states.

IV. SUMMARY

The nuclei ^{91}Sr and ^{92}Sr were produced at high spins as fission fragments following the fusion reaction ^{36}S+^{159}Tb at 165 MeV. γ rays were detected with the Gammasphere array. The level schemes of ^{91}Sr and ^{92}Sr were extended up to $E \approx 6$ MeV and $E \approx 8$ MeV, respectively. On the basis of a DCO analysis, spin assignments for high-spin states in the main sequences of both nuclei were made for the first time.

Excited states in ^{91}Sr and ^{92}Sr were interpreted in the framework of the spherical shell model. The calculations were performed in a model space including the proton orbitals $(0f_{5/2}, 1p_{3/2}, 1p_{1/2}, g_{9/2})$ and the neutron orbitals $(1p_{1/2}, 0g_{9/2}, 1d_{5/2})$. The calculations give a good overall description of the observed states. The negative-parity states in the main level sequence of ^{91}Sr are reproduced by the calculations mainly by the coupling of the $1d_{5/2}^3$ neutrons to proton configurations of the core nucleus ^{88}Sr. A change of the parity in the yrast sequence in ^{91}Sr and ^{92}Sr was suggested. The lowest-lying $11/2^-$ and $15/2^-$ states in ^{91}Sr and the 3^-, 5^-, and 7^- states in ^{92}Sr are described in the present calculations by coupling the proton excitations that create the octupole 3^- state of the core nucleus ^{88}Sr to the $1d_{5/2}^3$ and $1d_{5/2}^4$ neutrons, respectively. Based on a comparison with the $11/2^-$ state in ^{89}Sr, an influence of the $0h_{11/2}$ neutron orbital on these states is considered likely. The experimental findings hint to a possible reduction of the gap between the $1p_{3/2}$ and $1p_{1/2}$ proton orbitals in ^{92}Sr. The observed equidistant $\Delta J = 2$ level sequence on top of the 8^+ state, which resembles a vibrational-like sequence, could be well described by the configuration $\pi[(0f_{5/2}^{-2})(0g_{9/2}^2)]\nu(1d_{5/2}^4)$ that favors even spins.

ACKNOWLEDGMENTS

E.A.S. acknowledges financial support by the Bulgarian NRF under Contract Nos. PH 908 and MU-F-02/98, and by the Forschungszentrum Rossendorf. The group of the University of Tennessee acknowledges support by the U.S. Department of Energy under Contract No. DE-FG02-96ER40983. This work was supported by the U.S. Department of Energy, Nuclear Physics Division under Contract No. W-31-109-ENG-38.

[1] H. Mach, F. K. Wohn, G. Molnár, K. Sistemich, J. C. Hill, M. Moszyński, R. L. Gill, W. Krips, and D. S. Brenner, Nucl. Phys. **A523**, 197 (1991).
[2] H. Mach, M. Moszyński, R. L. Gill, F. K. Wohn, J. A. Winger, J. C. Hill, G. Molnár, and K. Sistemich, Phys. Lett. B **230**, 21 (1989).
[3] P. Federman, S. Pittel, and A. Etchegoyen, Phys. Lett. **140B**, 269 (1984).
[4] E. A. Stefanova, R. Schwengner, G. Rainovski, K. D. Schilling, A. Wagner, F. Dönau, E. Galindo, A. Jungclaus, K. P. Lieb, O. Thelen, J. Eberth, D. R. Napoli, C. A. Ur, G. de Angelis, M. Axiotis, A. Gadea, N. Marginean, T. Martinez, Th. Kröll, and T. Kutsarova, Phys. Rev. C **63**, 064315 (2001).
[5] S. E. Arnell, A. Nilsson, and O. Stankiewicz, Nucl. Phys. **A241**, 109 (1975).
[6] H. W. Müller and J. W. Tepel, Nucl. Data Sheets **54**, 1 (1988).
[7] H. P. Blok, W. R. Zimmerman, J. J. Kraushaar, and P. A. Batay-Csorba, Nucl. Phys. **A287**, 156 (1977).
[8] N. Fotiades, J. A. Cizewski, K. Y. Ding, R. Krucken, J. A. Becker, L. A. Bernstein, K. Hauschild, D. P. McNabb, W. Younes, P. Fallon, I. Y. Lee, and A. O. Macchiavelli, Phys. Scr. **T88**, 127 (2000).
[9] I. Y. Lee, Nucl. Phys. **A520**, 641c (1990).
[10] D. C. Radford, Nucl. Instrum. Methods Phys. Res. A **361**, 297 (1995).
[11] R. M. Steffen, and K. Alder, in *The Electromagnetic Interaction in Nuclear Spectroscopy*, edited by W. D. Hamilton (North-Holland, Amsterdam, 1975), p. 505.
[12] K. S. Krane, R. M. Steffen, and R. M. Wheeler, Nucl. Data Tables **11**, 351 (1973).
[13] A. Krämer-Flecken, T. Morek, R. M. Lieder, W. Gast, G. Hebbinghaus, H. M. Jäger, and W. Urban, Nucl. Instrum. Methods Phys. Res. A **275**, 333 (1989).
[14] W. Urban, M. A. Jones, C. J. Pearson, I. Ahmad, M. Bentaleb, J. L. Durell, M. J. Leddy, E. Lubkiewicz, L. R. Morss, W. R. Phillips, N. Schulz, A. G. Smith, and B. J. Varley, Nucl. Instrum. Methods Phys. Res. A **365**, 596 (1995).
[15] K. R. Pohyl, P. H. Regan, J. E. Bush, P. E. Raines, D. P. Balamuth, D. Ward, A. Galindo-Uribarri, V. P. Janzen, S. M. Mullins, and S. Pilotte, Phys. Rev. C **53**, 2682 (1996).
[16] E. A. Stefanova, R. Schwengner, J. Reif, H. Schnare, F. Dönau, M. Wilhelm, A. Fitzler, S. Kasemann, P. von Brentano, and W. Andrejtscheff, Phys. Rev. C **62**, 054314 (2000).
[17] C. M. Baglin, Nucl. Data Sheets **91**, 423 (2000).
[18] S. S. Ghugre, S. Naguleswaran, R. K. Bhowmik, U. Garg, S. B. Patel, W. Reviol, and J. C. Walpe, Phys. Rev. C **51**, 2809 (1995).
[19] S. S. Ghugre, S. B. Patel, M. Gupta, R. K. Bhowmik, and J. A. Sheikh, Phys. Rev. C **50**, 1346 (1994).
[20] B. Kharraja, S. S. Ghugre, U. Garg, R. V. F. Janssens, M. P. Carpenter, B. Crowell, T. L. Khoo, T. Lauritsen, D. Nisius, W. Reviol, W. F. Mueller, L. L. Riedinger, and R. Kaczarowski, Phys. Rev. C **57**, 2903 (1998).
[21] B. Kharraja, S. S. Ghugre, U. Garg, R. V. F. Janssens, M. P. Carpenter, B. Crowell, T. L. Khoo, T. Lauritsen, D. Nisius, W. Reviol, W. F. Mueller, L. L. Riedinger, and R. Kaczarowski, Phys. Rev. C **57**, 83 (1998).
[22] J. M. Chatterjee, M. Saha-Sarkar, S. Bhattacharya, P. Banerjee, S. Sarkar, R. P. Singh, S. Murulithar, and R. K. Bhowmik, Nucl. Phys. **A678**, 367 (2000).
[23] G. Winter, R. Schwengner, J. Reif, H. Prade, L. Funke, R. Wirowski, N. Nicolay, A. Dewald, P. von Brentano, H. Grawe, and R. Schubart, Phys. Rev. C **48**, 1010 (1993).
[24] G. Winter, R. Schwengner, J. Reif, H. Prade, J. Döring, R. Wirowski, N. Nicolay, P. von Brentano, H. Grawe, and R. Schubart, Phys. Rev. C **49**, 2427 (1994).

[25] R. Schwengner, G. Winter, J. Reif, H. Prade, L. Käubler, R. Wirowski, N. Nicolay, S. Albers, S. Eßer, P. von Brentano, and W. Andrejtscheff, Nucl. Phys. **A584**, 159 (1995).
[26] R. Schwengner, J. Reif, H. Schnare, G. Winter, T. Servene, L. Käubler, H. Prade, M. Wilhelm, A. Fitzler, S. Kasemann, E. Radermacher, and P. von Brentano, Phys. Rev. C **57**, 2892 (1998).
[27] X. Ji and B. H. Wildenthal, Phys. Rev. C **37**, 1256 (1988).
[28] R. Gross and A. Frenkel, Nucl. Phys. **A267**, 85 (1976).
[29] P. C. Li, W. W. Daehnick, S. K. Saha, J. D. Brown, and R. T. Kouzes, Nucl. Phys. **A469**, 393 (1987).
[30] J. Blomqvist and L. Rydström, Phys. Scr. **31**, 31 (1985).
[31] D. H. Gloeckner and F. J. D. Serduke, Nucl. Phys. **A220**, 477 (1974).
[32] D. Zwarts, Comput. Phys. Commun. **38**, 365 (1985).